Optical properties of dislocations in wurtzite ZnO single crystals introduced at elevated temperatures

Y. Ohno,[1,a] H. Koizumi,[1] T. Taishi,[1] I. Yonenaga,[1] K. Fujii,[2] H. Goto,[2] and T. Yao[2]
[1]*Institute for Materials Research, Tohoku University, Katahira 2-1-1, Aoba-ku, Sendai 980-8577, Japan*
[2]*Center for Interdisciplinary Research, Tohoku University, Aramaki aza Aoba 6-3, Aoba-ku, Sendai 980-8578, Japan*

(Received 4 May 2008; accepted 10 July 2008; published online 6 October 2008)

Optical properties of wurtzite ZnO bulk single crystals in which an arbitrary number (typically 10^9-10^{10} cm^{-2}) of fresh dislocations were introduced intentionally by the plastic deformation at elevated temperatures (923–1073 K) were examined. Deformed specimens showed excitonic light emission with photon energies of 3.100 and 3.345 eV, as well as their LO phonon replicas at 11 K. The light intensities increased with increasing dislocation density. The activation energy for a thermal quenching of the 3.100 or 3.345 eV emission band, which corresponds to the depth of the localized energy level associated with the emission band, was estimated to be 0.3 ± 0.1 or 0.05 ± 0.01 eV, respectively. The origin of the energy levels was proposed as point defect complexes involving dislocations. The introduction of the dislocations at the elevated temperatures above 923 K did not influence the intensities of the emission bands except the dislocation-related emission bands. © *2008 American Institute of Physics*. [DOI: 10.1063/1.2977748]

I. INTRODUCTION

ZnO has a wide direct band gap of 3.37 eV and large exciton binding energy of 60 meV at room temperature, rather large in comparison with GaN, and the excitonic emission at elevated temperatures up to 550 K has been demonstrated.[1] Consequently, ZnO has rapidly emerged as a promising analog to GaN for optoelectronic devices employing excitonic effects in the short wavelength range. Also, several other characteristics, such as potential ferromagnetism, further enhance the interest in this material for manufacturing future nanodevices.

Despite considerable success in optimizing the growth conditions and structural quality, ZnO epitaxial layers still contain a high density of defects that influence their optoelectronic properties. Most characteristic defects investigated by transmission electron microscopy (TEM) are high-density (typically 10^9-10^{11} cm^{-2}) dislocations passing through the entire layers.[2] In ZnO, dislocations are introduced with lower stress and are highly mobile in comparison with those in GaN.[3] It has been considered that they are easily introduced during device fabrication as well as crystal growth. As reported in a large number of studies in GaN, it is known that dislocations can influence the device performance through nonradiative recombination. Thus, the knowledge of the influence of dislocations is required for the practical use of this material. Even though ZnO has the same crystal structure as GaN, the influence of dislocations in ZnO has not been fully elucidated. Cathodoluminescence spectroscopy in a scanning electron microscope,[4–7] scanning capacitance microscopy,[8] and electron holography combined with TEM,[9] have suggested that localized energy levels exist near the dislocations. It has been proposed that several emission bands peaking at photon energies of 3.33,[10] 3.314,[11] and ~3.1 eV (Refs. 12 and 13) are related to extended defects including the dislocations, even though the relationships are controversial.

So far, most works have concentrated only on the optical properties of the dislocations introduced at room temperature. Preliminary studies of our group showed that the dislocations newly introduced by plastic deformation at elevated temperatures, comparable to the typical temperatures for the fabrication of ZnO-based devices, induce dislocation-related emission bands.[14] In the present work, the optical properties of the dislocations are systematically investigated. It is shown that they act as radiative recombination center, while the dislocations introduced at room temperature act as nonradiative one. Two dislocation-related emission bands are found, and the energy levels associated with the emission bands are quantitatively estimated. The origin of the energy levels is discussed in terms of the reaction of dislocations and point defects at elevated temperatures be a key to elucidate the influence of dislocations and point defects on the optoelectronic properties of semiconductors.

II. EXPERIMENTS

Samples were wurtzite ZnO bulk single crystals with an *n*-type carrier concentration of 5×10^{13} cm^{-3} at room temperature purchased from Goodwill (Russia). The density of grown-in dislocations was estimated to be 10^4 cm^{-2} by the etch pit technique, and no dislocation was indeed observed in a small volume (about 10^{-8} cm^3) by TEM [e.g., Fig. 1(a)].

Rectangular specimens, $2\times2\times7$ mm^3 in size, were sectioned from a crystal, and they were introduced fresh dislocations by annealing under compressive stress. The compressive axis was inclined at 45° with respect to the [0001] direction, with the surface of one side parallel to the $(10\bar{1}0)$ plane. Compression tests were conducted in a flowing high-purity argon gas atmosphere at temperatures of 923–1123 K, under a constant shear strain rate of 4×10^{-4} s^{-1}, and up to the strain of about 30%. Details of the compression process

[a]Electronic mail: yutakaohno@imr.tohoku.ac.jp.

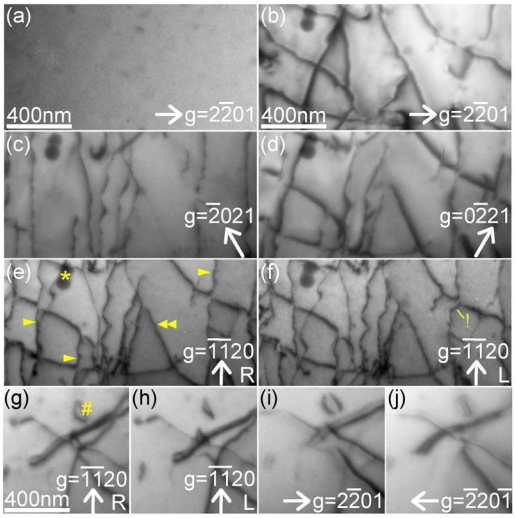

FIG. 1. (Color online) Two-beam bright-field TEM images of a specimen: (a) as-grown, [(b)–(f)] deformed at 1023 K, and [(g)–(j)] deformed at 1123 K (*g* diffraction condition). The thickness of the specimens is about 300 nm. (e) and (f), or (g) and (h), are a pair of stereo micrographs taken with an electron beam inclined by ±12° from [0001] toward [1$\bar{1}$00]. A single or double arrowhead in (e) indicates a screw or edge dislocation component, respectively. The "!" mark in (f) and the "#" mark in (g) indicate a jog and a dislocation loop of interstitial type, respectively. The asterisk mark in (e) indicates a marker.

were published elsewhere.[3] Some specimens were only heated at the above-mentioned temperatures without any deformation.

The structural nature was characterized by TEM with a 120-keV electron beam. Under the beam irradiation, the effect of the radiation enhanced dislocation motion[7] seemed to be small. The dislocation density, defined as the total length of the dislocation lines existing in a unit volume, was estimated by three-dimensional TEM (a so-called stereo microscopy).

The optical property was characterized by photoluminescence (PL) spectroscopy for the specimens deformed at 923–1073 K and those heated at the same temperatures without stress. The specimens were illuminated with a 325 nm laser light (with the probe size of 0.015 mm diameter) from a 15 mW He-Cd laser. PL spectra were obtained at the temperature T of 11 K, otherwise it is noted in the text. The excitation power density P was 35 W cm^{-2}, otherwise it is noted in the text. PL lights were collected into a photomultiplier tube detector through a 32 cm monochromator, and the spectral resolution was about 0.4 meV.

III. RESULTS

A. Introduction of fresh dislocations

In deformed specimens, dislocations of high density more than 10^8 cm^{-2} were introduced. A conventional two-beam TEM method, as shown in Figs. 1(b)–1(f), revealed that no dislocation was dissociated[15] and that the Burgers vector of the dislocations was $(a/3)[11\bar{2}0]$, $(a/3)[2\bar{1}\bar{1}0]$, or $(a/3)[1\bar{2}10]$. There existed a screw [indicated with a single arrowhead in Fig. 1(e)], edge [the double arrowhead in Fig. 1(e)], and mixed dislocations and the ratio of the dislocation densities for the screw, edge, and mixed dislocations was about 5:1:14 irrespective of the deformation temperature. Many dislocations passed through the specimens with the rest forming dislocation loops [e.g., "#" in Fig. 1(g)]. Three-dimensional TEM observation [e.g., Figs. 1(e) and 1(f)] revealed that many parts of the dislocations lay on a (0001) basal plane, with the rest lying on a plane inclined with respect to the {0001} planes (most likely one of the {10$\bar{1}$1} pyramidal planes).[17] The dislocation loops were identified as being interstitial-type by the inside-outside contrast method, as seen in Figs. 1(g)–1(j).[18] Many dislocations contained jogs [e.g., "!" in Fig. 1(f)], indicating that a high density of point defects would be introduced via the climb motion of the dislocations. Other types of extended defects, such as twins and stacking faults, were not observed by TEM.

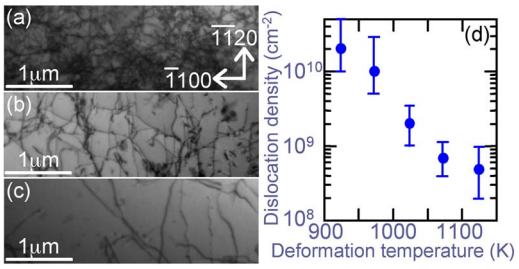

FIG. 2. (Color online) TEM images of a specimen deformed at (a) 923 K, (b) 1023 K, and (c) 1123 K. The thickness of the specimens is about 300 nm. (d) The total dislocation density vs the deformation temperature.

The total dislocation density, defined as the sum of the dislocation densities for the three kinds of dislocations, decreased with increasing the deformation temperature (Fig. 2). The density ranged from $\sim 5\times 10^{10}$ to $\sim 2\times 10^{8}$ cm^{-2} in the temperature range of 923–1123 K.

B. Effects of dislocations on optical properties

Figure 3 shows a typical PL spectrum obtained from a specimen deformed at a temperature of 923 K, as well as that from an undeformed specimen that was annealed at the same temperature without stress. Both specimens exhibited near-band edge emissions due to free excitons [peaking at 3.390 eV (FX_B) and 3.378 eV (FX_A)],[19] excitons bound to neutral donors [3.373 eV ($D_2^0X_B$), 3.361 eV ($D_2^0X_A$), and 3.323 eV two-electron satellite (TES)],[19] excitons bound to neutral acceptors [3.354 eV ($A_1^0X_A$)],[19] donor-acceptor pairs (DAP) [3.217 eV],[19] unknown defects [3.335 eV (d1) (Ref. 10) and 3.314 eV (d2) (Ref. 11)], as well as their longitudinal-optical (LO) phonon replicas. Also, deep level emissions due to the green (2.43 eV), yellow (2.18 eV), and red (1.91 eV) emission bands previously reported in Ref. 19 were observed. The intensity of the emission lines for the deformed specimen I_{deformed} and that for the undeformed one $I_{\text{undeformed}}$ was examined,[14] and the intensity ratio $R=I_{\text{deformed}}/I_{\text{undeformed}}$ was ~ 1 for the above-mentioned emission lines [Fig. 3(a)], even though an excitonic emission line for the deformed specimen was slightly narrow in comparison with the undeformed one. Similar results were obtained irrespective of the deformation temperature. This indicates that (1) the above-mentioned emission lines are not related to dislocations or deformation

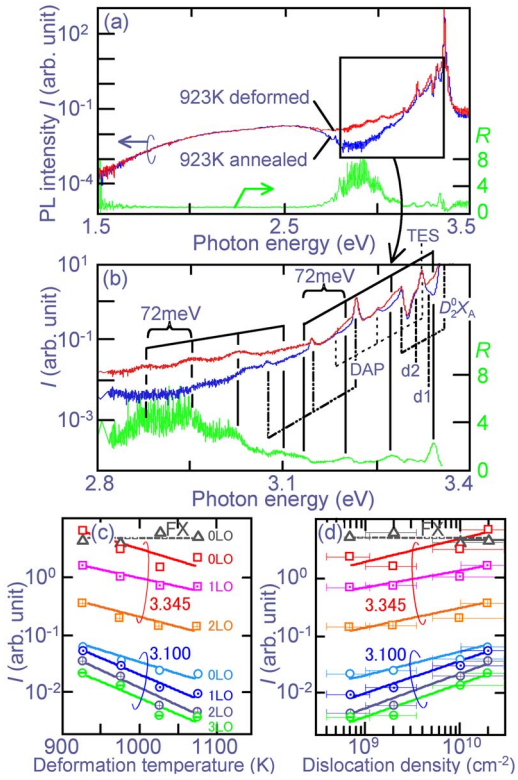

FIG. 3. (Color online) (a) The logarithmic PL intensity vs the photon energy for a specimen deformed at 923 K or annealed at 923 K without stress. The ratio of those PL intensities, $R=I_{\text{deformed}}/I_{\text{undeformed}}$, is also shown. A part of (a) is magnified in (b). The PL intensity at the peak energy of a LO phonon line as a function of (c) the deformation temperature or (d) the total dislocation density. The squares, circles, and triangles show the data for the 3.345 eV, 3.100 eV, and FX_A emission bands, respectively. The open marks, the marks with dots, those with "+" and "-," show the data for the zero-, one-, two-, and three-LO phonon lines, respectively.

induced defects and that (2) the optical properties of the emission lines are not affected by the dislocations introduced at the elevated temperatures.

In the deformed specimens, additional emission lines peaking at 3.100 and 3.345 eV, as well as their LO phonon replicas (with the separation between the nearest-neighbor emission lines of 72 meV), were observed. These lines were clearly observable in a spectrum of the intensity ratio R versus the photon energy [e.g., Fig. 3(b)]. The intensity of an emission line for the 3.100 and 3.345 eV emission bands decreased monotonously with increasing the deformation temperature, while that for other emission bands, such as the FX_A emission band, was independent of the deformation temperature [Fig. 3(c)]. From the data in Figs. 2(d) and 3(c), it is concluded that the intensity for the 3.100 and 3.345 eV emission bands increases monotonously with increasing the total dislocation density [Fig. 3(d)]. High intensity of those emission bands was indeed obtained from a specimen in which a number of dislocations should be located.[14] The introduction of dislocations at the elevated temperatures, therefore, results in the formation of those emission bands.

C. Localized energy levels associated with dislocation-related emission bands

The temperature T-dependent intensity of an emission line can be fitted with a function[20]

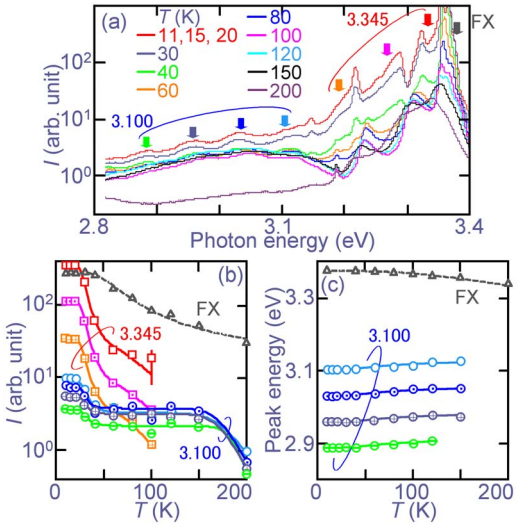

FIG. 4. (Color online) (a) PL spectra for a deformed specimen (the deformed temperature; 923 K) obtained at various temperatures T. T dependence of (b) the peak intensity and (c) the photon energy of a LO phonon line. The meaning of the marks is the same as in Fig. 3(c).

$$I(T) = I_0/[1 + C_0 \exp(\Delta E_0/kT)], \tag{1}$$

where ΔE_0 is the activation energy for the thermal quenching process and I_0 or C_0 is a constant. An intensity for the FX_A emission band followed the relationship, as seen in Fig. 4(b), and the activation energy was estimated to be 0.02 ± 0.01 eV, comparable to that reported previously.[21] On the other hand, an intensity for the 3.100 and 3.345 eV emission bands decreased via two thermal quenching processes. It could be fitted with a function

$$I(T) = I_0/[1 + C_0 \exp(\Delta E_0/kT)] + I_1/[1 + C_1 \exp(\Delta E_1/kT)]. \tag{2}$$

The activation energy for the quenching process arose at lower temperatures (first process) and that rises at higher temperatures (second process), ΔE_0 and ΔE_1, respectively, were estimated as 0.02 ± 0.01 and 0.3 ± 0.1 eV for the 3.100 eV emission band and 0.02 ± 0.01 and 0.05 ± 0.01 eV for the 3.345 eV emission band.

The peak energy of an emission line normally decreases with increasing T due to the thermal expansion of the lattice constant, and it can be fitted with a function[22]

$$E(T) = E_0 + A/[\exp(E_{\text{phonon}}/kT) - 1], \tag{3}$$

where E_0, A, or E_{phonon} is a constant [e.g., see the data for an emission line of the FX_A emission band in Fig. 4(c)]. However, the peak energies of the 3.100 eV emission band increased monotonously with increasing T in the temperature range of 11–150 K [Fig. 4(c)].[23] A peak energy at $T = 100$–150 K was ~0.02 eV larger than that at 11–20 K.

The activation energy ΔE_0 for the 3.100 eV emission band was the same as that for the FX_A emission band (0.02 eV), and a peak energy of the 3.100 eV emission band increased by the same amount of ΔE_0 after the first quenching process. Therefore, it was considered that (1) ΔE_0 corresponded to the binding energy of excitons at a localized energy level and (2) the first quenching process was due to the

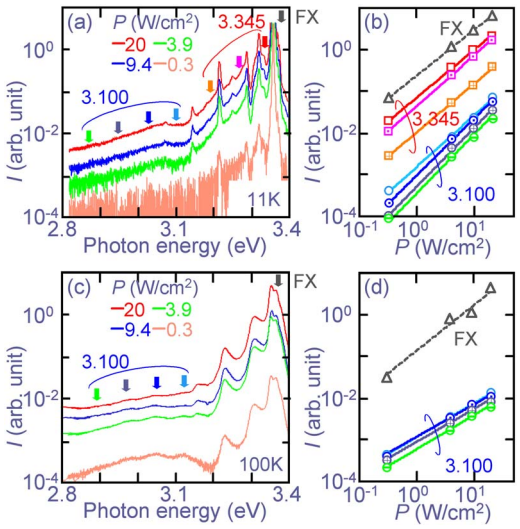

FIG. 5. (Color online) PL spectra for a deformed specimen (the deformed temperature: 973 K) at several excitation power densities P obtained at (a) 11 K or (c) 100 K. P-dependent PL intensity for a LO phonon line obtained at (b) 11 K or (d) 100 K. The meaning of the marks is the same as in Fig. 3(c).

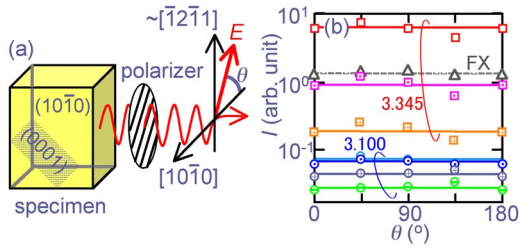

FIG. 6. (Color online) (a) The experimental setup for linear polarization measurement. The transmission direction of the electric field E for a PL light is determined by the rotation angle of the polarizer θ. (b) θ-dependent PL intensity of a LO phonon line at $T=11$ K for a deformed specimen (the deformed temperature; 923 K). The meaning of the marks is the same as in Fig. 3(c).

transition from an excitonic recombination at the level to a recombination between the level and a band (a bound-to-free transition). In order to confirm the above hypothesis, excitation power density P-dependent peak intensities of the emission band were studied at the temperatures before (at 11 K) and after (at 100 K) the first quenching process [Figs. 5(a) and 5(c)]. An intensity was fitted with a function

$$I(P) = I_0 P^{\alpha}, \tag{4}$$

where I_0 or α was a constant and α was estimated to be about 1.3 at $T=11$ K [Fig. 5(b)]. Since the estimated value was in the range of 1.0–2.0, the origin of the emission was excitonic recombination,[24] similar to the FX_A emission [$\alpha=1.1$, see Fig. 5(b)], at this temperature. On the other hand, at $T=100$ K, α decreased to about 0.8, unlike the FX_A emission ($\alpha=1.1$) [Fig. 5(d)]. Since the estimated value was less than 1.0, the origin of the emission was a recombination via a localized energy level,[25] i.e., a recombination between a localized level and a band or a donor-acceptor pair recombination. Since the peak energies of the emission band did not depend on P [Fig. 5(c)], the latter possibility was excluded. It is therefore concluded that the first quenching process of the 3.100 eV emission band is due to a bound-to-free transition. Similarly, the first quenching process of the 3.345 eV emission band might be due to a bound-to-free transition, since ΔE_0 was also the same as that for the FX_A emission band (0.02 eV) and α was in the range of 1.0–2.0 (about 1.2) at $T=11$ K [Fig. 5(b)].

The difference of the zero-phonon peak energies for the FX_A emission band and the 3.100 eV one corresponded to the ΔE_1 for the 3.100 eV one, i.e., 3.378 eV−3.100 eV =0.278 eV at $T=11$ K. Also, the difference for the FX_A emission band and the 3.345 eV one was close to the ΔE_1 for the 3.345 eV one, i.e., 3.378 eV−3.345 eV=0.033 eV at $T=11$ K. These results indicate that the second quenching attributes to thermal escape of the trapped carriers in the localized energy levels associated with the 3.100 and 3.345 eV emission bands. In other words, ΔE_1 corresponds to the depth of the localized energy levels. Therefore, the levels associated with the 3.100 and 3.345 eV emission bands are, respectively, estimated to be 0.3 ± 0.1 and 0.05 ± 0.01 eV in depth.

D. The origin of the dislocation-related localized energy levels

The relative intensity of the nth phonon replicas, I_n, can be written as[26]

$$I_n = I_0(S^n/n!)(n=0,1,2,\ldots), \tag{5}$$

where S is the Huang–Rhys factor according to the Franck–Condon model. The factors for the 3.100 and 3.345 eV emission bands were, respectively, estimated to be 1.4 and 0.2. They differed from the factors for other emission bands in our specimens, including near-band edge emissions (e.g., 0.01–0.04 for the $D_2^0X_A$ emission[27]) and deep level emissions (e.g., 6.5 for the green emission[28]). Also, they differed from the factors for the 3.2108 eV emission band (~0.5),[29] which were induced by deformation at room temperature but were not induced in our specimens deformed at elevated temperatures above 923 K.

Many dislocations in various semiconductors form deep levels and they act as nonradiative recombination centers. On the other hand, some dislocations, such as 90° Shockley partials in ZnSe,[30] induce dislocation-related radiative centers and they emit light linearly polarized parallel to the dislocation cores. So, the polarization of a PL light for the 3.100 and 3.345 eV emission bands was investigated. Since all PL lights were polarized along the c axis due to the effect of spontaneous polarization of the host ZnO crystal, PL spectra were obtained with the experimental setup shown in Fig. 6(a) in order to reduce the effect. No obvious polarization was observed for those emission lines, as well as for FX_A emission line [Fig. 6(b)]. This suggests that point defects (i.e., interstitial atoms or vacancies) introduced with dislocations, rather than dislocation cores, are the candidates for the origin of the localized energy levels associated with the 3.100 and 3.345 eV emission bands.

IV. DISCUSSION

The effects of dislocations on optical properties have been studied for the dislocations introduced at room temperature by mechanical milling[12,29] or indentation.[4,5,17,31] According to the works, (1) the intensity of near-band edge emissions decreases,[4,5,12,17] while (2) that of deep level emissions (e.g., the yellow emission band that could be associated with Zn vacancies)[32] increases.[4,12] (3) The 3.2108 eV emission band (presumably due to pairs of a Zn-vacancy acceptor and a Zn-interstitial donor)[29] is induced[12,29] and (4) no dislocation-related emission band is observed. These results indicate that the dislocations act as nonradiative recombination centers, and point defects that are responsible to deep level emissions are also introduced with the dislocations. The dislocations introduced at room temperature are, therefore, far different from those induced above 923 K. Specifically, our present results indicate that the intensities of deep level emissions, as well as near-band edge emissions, are unchanged after the introduction of the latter dislocations. This suggests that the dislocations may not act as nonradiative recombination centers or that the introduction of the dislocations may result in cancelling of multiple recombination processes.

When the specimens with the dislocations introduced at room temperature are annealed at temperatures above 873 K, (5) the intensity of near-band edge emissions measurably recovers,[4] while (6) that of deep level emissions decreases.[4,31] (7) An emission band with a photon energy around 3 eV, similar to the 3.100 eV emission band, is induced by annealing above 773 K.[31] Namely, as the nonradiative recombination centers and point defects are annealed out, an emission band similar to the 3.100 emission band is formed. The type of the dislocations introduced at room temperature[17] is similar to that introduced at elevated temperatures. These results suggest that the origin of the 3.100 and 3.345 eV emission bands is formed by the reaction of dislocations and point defects via thermal migration of point defects at the elevated temperatures, i.e., the atomistic structure nearby the cores of the dislocations introduced at elevated temperatures would differ from that introduced at room temperature. Actually, transmission electron holography has revealed that localized energy levels exist near dislocations in a ZnO layer grown at 653 K, and that the origin of the levels is related to point defects in the vicinity of the dislocations rather than to the dislocation cores.[9] The 3.100 and 3.345 eV emission bands are not observed in the specimens annealed after ion implantation,[32] indicating that they are not formed only by the introduction of point defects. Therefore, the origin of those emission bands is probably point defect complexes involving dislocations, even though their atomistic structure remains obscure.

It is interesting to note that the introduction of dislocations at elevated temperatures does not influence the intensities of the emission bands except the dislocation-related bands, suggesting that the reaction of dislocations and point defects results in the suppression of nonradiative recombination centers. This characteristic of ZnO may be an advantage over GaN. Indeed, GaN exhibits a phenomenon that all intensities decrease with the introduction of dislocations introduced even at elevated temperatures,[33] as well as at room temperature.[34]

V. CONCLUSION

PL spectroscopy combined with TEM revealed that (1) the dislocations freshly introduced by plastic deformation at elevated temperatures above 923 K induce two emission bands with the zero-phonon peak energies of 3.100 and 3.345 eV and that (2) the emissions arise via the localized energy levels with the depths of 0.3 ± 0.1 and 0.05 ± 0.01 eV. It was suggested that the origin of the levels is point defect complexes involving the dislocations. The dislocations, introduced at the elevated temperatures, did not influence the intensities of the emission bands except the dislocation-related emission bands.

ACKNOWLEDGMENTS

This work was partially supported by the Ministry of Education, Culture, Sports, Science, and Technology, Japan, a Grant-in-Aid for Scientific Research (B), [Grant No. 19310072 (2007–2009)].

[1] D. M. Bagnall, Y. F. Chen, Z. Zhu, T. Yao, M. Y. Shen, and T. Goto, Appl. Phys. Lett. **73**, 1038 (1998).
[2] e.g., A. Setiawan, Z. Vashaei, M. W. Cho, T. Yao, H. Kato, M. Sano, K. Miyamoto, I. Yonenaga, and H. J. Ko, J. Appl. Phys. **96**, 3763 (2004).
[3] I. Yonenaga, H. Koizumi, T. Taishi, and Y. Ohno, J. Appl. Phys. **103**, 093502 (2008).
[4] V. A. Coleman, J. E. Bradby, C. Jagadish, and M. R. Phillips, Appl. Phys. Lett. **89**, 082102 (2006).
[5] Z. Takkouk, N. Brihi, K. Guergouri, and Y. Marfaing, Physica B (Amsterdam) **366**, 185 (2005).
[6] S. Vasnyov, J. Schreiber, and L. Hoering, J. Phys.: Condens. Matter **16**, 269 (2004).
[7] K. Maeda, K. Suzuki, Y. Yamashita, and Y. Mera, J. Phys.: Condens. Matter **12**, 10079 (2000).
[8] W.-R. Liu, W. F. Hsieh, C.-H. Hsu, K. S. Liang, and F. S.-S. Chien, J. Cryst. Growth **297**, 294 (2006).
[9] E. Muller, D. Gerthsen, P. Bruckner, F. Scholz, Th. Gruber, and A. Waag, Phys. Rev. B **73**, 245316 (2006).
[10] H. Alves, D. Pfisterer, A. Zeuner, T. Riemann, J. Christen, D. M. Hofmann, and B. K. Meyer, Opt. Mater. (Amsterdam, Neth.) **23**, 33 (2003).
[11] M. Schirra, R. Schneider, A. Reiser, G. M. Prinz, M. Feneberg, J. Biskupek, U. Kaiser, C. E. Krill, R. Sauer, and K. Thonke, Physica B (Amsterdam) **401–402**, 362 (2007).
[12] R. Radoi, P. Fernandez, J. Piqueras, M. S. Wiggins, and J. Solos, Nanotechnology **14**, 794 (2003).
[13] A. Urbieta, P. Fernandez, J. Piqueras, Ch. Hardalov, and T. Sekiguchi, J. Phys. D **34**, 2945 (2001).
[14] Y. Ohno, H. Koizumi, T. Taishi, I. Yonenaga, K. Fujii, H. Goto, and T. Yao, Appl. Phys. Lett. **92**, 011922 (2008).
[15] Even though a dislocation is believed to be dissociated with dissociation width of less than 2 nm (Ref. 16), it is difficult to detect under the present experimental condition.
[16] K. Suzuki, M. Ichihara, and S. Takeuchi, Jpn. J. Appl. Phys., Part 1 **33**, 1114 (1994).
[17] J. E. Bradby, S. O. Kucheyev, J. S. Williams, C. Jagadish, M. V. Swain, P. Munroe, and M. R. Phillips, Appl. Phys. Lett. **80**, 4537 (2002).
[18] P. B. Hirsch, A. Howie, R. B. Nicholson, D. W. Pashley, and M. J. Whelan, *Electron Microscopy of Thin Crystals* (Butterworth, London, 1965), Chap. 11.
[19] As a review, U. Ozgur, Y. I. Alivov, C. Liu, A. Teke, M. A. Reshchikov, S. Doian, V. Avrutin, S. J. Cho, and H. Morkoc, J. Appl. Phys. **98**, 041301 (2005).
[20] e.g., P. O. Holtz, B. Monemar, and H. J. Lozykowski, Phys. Rev. B **32**, 986 (1985).

[21]A. B. M. A. Ashrafi, N. T. Binh, B. P. Zhang, and Y. Segawa, J. Appl. Phys. **95**, 7738 (2004).
[22]H. Y. Fan, Phys. Rev. **82**, 900 (1951).
[23]The peak energies for the 3.100 eV emission band at $T=200$ K, as well as those for the 3.345 eV emission band at $T=30-200$ K, were not obtained quantitatively due to large experimental error.
[24]For example, T. Schmidt, K. Lischka, and W. Zulehner, Phys. Rev. B **45**, 8989 (1992).
[25]For example, Z. C. Feng, A. Mascarenhas, and W. J. Choyke, J. Lumin. **35**, 329 (1986).
[26]K. Huang and A. Rhys, Proc. R. Soc. London, Ser. A **204**, 406 (1950).
[27]H.-C. Hsu, Y.-K. Tseng, H.-M. Cheng, J.-H. Kuo, and W.-F. Hsieh, J. Cryst. Growth **261**, 520 (2004).
[28]S. L. Shi, G. Q. Li, S. J. Xu, Y. Zhao, and G. H. Chen, J. Phys. Chem. B **110**, 10475 (2006).
[29]D. W. Hamby, D. A. Lucca, and M. J. Klopfstein, J. Appl. Phys. **97**, 043504 (2005).
[30]U. Hilpert, J. Schreiber, L. Worschech, L. Horing, M. Ramsteiner, W. Ossau, and G. Landwehr, J. Phys.: Condens. Matter **12**, 10169 (2000).
[31]K. Yoshino, M. Yoneta, and I. Yonenaga, J. Mater. Sci.: Mater. Electron. **19**, 199 (2008).
[32]Q. X. Zhao, P. Klason, M. Willander, H. M. Zhong, W. Lu, and J. H. Yang, Appl. Phys. Lett. **87**, 211912 (2005).
[33]I. Yonenaga, H. Makino, S. Itoh, T. Goto, and T. Yao, J. Electron. Mater. **35**, 717 (2006).
[34]e.g., S. O. Kucheyev, J. E. Bradby, J. S. Williams, C. Jagadish, M. Toth, M. R. Phillips, and M. V. Swain, Appl. Phys. Lett. **77**, 3373 (2000).